J. Phys. Chem. C 116 (2012) 18884−18890 (doi: 10.1021/jp306160c).

Modeling with Hybrid DFT the Electronic Band Alignment at the Zinc Oxide-Anatase Interface

José C. Conesa

Instituto de Catálisis y Petroleoquímica, CSIC

Campus de Excelencia UAM-CSIC

Marie Curie 2, L10, Cantoblanco, 28049 Madrid, Spain

Phone: +34-915854766; fax: +34-915854760; e-mail: jcconesa@icp.csic.es

Abstract

The band alignment at semiconductor interfaces can be theoretically computed using periodic slab models together with hybrid functional DFT methods in which HF exchange mixing coefficients are properly chosen (as justified by their relationship with the dielectric constant) and the calculated electrostatic potential inside each slab is used as reference for the band edge energies. This principle is applied here to the interface between wurtzite-type ZnO and anatase-type TiO_2, two oxides with nearly identical band gap widths. According to the results, in a composite of both materials the conduction and valence bands of ZnO will lie ca. 0.3 eV lower in energy than those of anatase, influencing the way in which photogenerated electrons and holes will be routed in photocatalytic or photovoltaic systems which include interfaces between these two oxides. The performance improvement observed in dye-sensitized solar cells based on a nanostructured ZnO electrode when the surface of the latter is covered by a thin TiO_2 layer is thus justified. The system may serve as example for the estimation of the band alignment in other semiconductor junctions of interest in different kinds of devices.

Keywords: Exchange coefficient, ZnO, TiO_2, photocatalyst, electronic structure, band offset

Introduction

Interfaces between semiconductors have great importance in the behavior of a number of materials and devices, e.g. ceramics, sensors, photovoltaic cells, (opto)electronic components and (photo)catalysts. In many of these systems the relative positions of the electronic bands existing at both sides of the interface have great influence on that behavior, as they determine whether electrons will cross the interface in one or other direction either spontaneously or under the influence of an external stimulus like temperature gradients, mechanic deformations or electromagnetic fields. Such band alignment characteristics have been subject of many studies; these can be experimental, being based e.g. on spectroscopies (like XPS/UPS[1,2,3] or the STM-based ones[4,5]) or on the measurement of I-V curves[6,7], or theoretical, where different more or less sophisticated approaches can be followed in the calculations[8,9,10,11].

While extensive band alignment studies have been carried out involving the semiconductors that are used typically in electronic or photovoltaic devices, as e.g. silicon, III-V compounds, chalcogenides like those used in thin film photovoltaics or transparent conducting or high-k insulating oxides, they have progressed to a lower extent in the case of photocatalysts in spite of the importance of such alignment, recognized especially in the last years, for maximizing the efficient separation of photogenerated carriers which is needed to achieve a high yield of the chemical reaction of interest, be it the destruction of pollutants or the production of solar fuels[12,13]. This is probably connected with the fact that these systems are less frequently studied in the single crystal or compact thin layer form which is better adapted to advanced spectroscopic measurements.

One such system is, for example, that formed by the two paradigmatic photocatalysts TiO_2 (in its more photoactive form, anatase) and ZnO. These semiconductors have very

similar band gaps; at temperatures close to 0 K the optical gaps are 3.42 eV for anatase[14] and 3.44 eV for ZnO[15], while at ambient temperatures they are respectively close to 3.2 and 3.3 eV. Several works in the literature have studied photocatalysts constituted by anatase-ZnO composites and in several of them photoactivity improvements in comparison with the single phases have been reported[16,17,18,19,20,21,22]. In these cases it is normally hypothesized that the interface between both oxides can facilitate the separation of electrons and holes, and thus minimize unwanted recombination, if due to the relative band positions one of the photogenerated current carriers tends to go to one of the phases and the other carrier to the other phase, with the subsequent improvement in the process efficiency. However, there is disagreement concerning whether the bands of anatase would lie at higher or lower energy than those of ZnO[16,17,23,24,25,26], the arguments on this subject being usually based on data about the work function or flatband potential of the individual oxides. Although there are some measurements of the band alignment at the ZnO-rutile interface[27], to this author's knowledge no experimental or theoretical work has been done which allows determining the band alignment between ZnO and anatase in a situation in which they are in direct contact.

The present work addresses this issue by means of quantum mechanical calculations applied to periodic slab models of the interface. Hybrid density functional theory is used for this; as will be shown below, this requires counteracting with special schemes the known shortcomings of the present theory, so that one may reach a reasonably reliable result, which in this case predicts that in a composite of both oxides the ZnO bands will lie a few tenths of eV below those of anatase-type TiO_2.

Models and methods

The interface model(s)

The interface will be represented here by periodically alternating slabs of the two oxides. One fundamental condition that should be followed in building such model is that the terminating surface of each slab should be electrically neutral; if possible it should also be smooth and have a low surface energy. For anatase the surface known to be most stable among those with low Miller indices is the (101) one, neutral although not very smooth, as it presents rather a stepped shape; other neutral surfaces like (001) and (100) are smoother and known to be also stable. For ZnO stable neutral surfaces are (110) and (1 -1 0), and indeed this oxide grows frequently in form of long hexagonal columns parallel to the *c* axis[28], the sides of which are formed by these surfaces. Surface (001), which can be prepared experimentally as well, has however a polar character which introduces electrostatic complications in an infinite periodic model; it will not be used here. In addition it should be possible to superimpose the periodicities of the slab surfaces of both oxides with a satisfactory epitaxial match.

Here it is fortunate that such an adequate match exists between two nonpolar and reasonably flat surfaces of these oxides: the (110) surface of ZnO has a 2D rectangular cell of 5.63x5.21 Å size, while the (001) surface of anatase has a $\sqrt{2}$x$\sqrt{2}$ square 2D supercell with dimensions 5.35x5.35 Å. It is also possible to align the structures of both slabs (once distorted so that the 2D surface lattice dimensions are equal) so that most of the undercoordinated atoms in their surfaces are able to form additional M-O bonds across the interface, completing thus their coordination spheres. Fig. 1 shows a model built in this way, and which will be the basis of the calculations carried out here; the ZnO and anatase slabs forming it, having thicknesses of ca. 18.0 and 21.3 Å, have respectively 11 and 9 atomic layers and Zn_2O_2 and Ti_2O_4 atomic composition per surface unit cell in each layer; the total contents of the resulting unit cell is thus

$Zn_{22}Ti_{18}O_{58}$. It is worth noting that this structure has rather low symmetry, but that the only symmetry element existing, a 2-fold screw axis parallel to the interface (perpendicular to the drawing plane in Fig. 1) which leads to a $P2_1$ monoclinic space group, ensures that both interfaces are equivalent by symmetry so that in the cell the component of the overall electric dipole moment perpendicular to the interface is zero (the component at one interface is balanced by that at the other one). To check the dependence of the results on the slab sizes some additional calculations were made with smaller models containing respectively 7+5 layers (i.e. with a composition $Zn_{14}Ti_{10}O_{34}$ in the unit cell) and 9+9 layers (i.e. a $Zn_{18}Ti_{18}O_{54}$ composition), both of them having the same $P2_1$ symmetry and interface type as the model with 11+9 layers.

Calculation Methods

Initial geometry relaxations were made at the GGA level (functional PBE) on the slab models and on the individual oxides using program VASP[29], which expands the wavefunctions and electronic densities in plane waves, and representing with the PAW method[30] the inner electronic cores, which included 18, 12 and 2 electrons for Zn, Ti and O respectively. The plane wave energy cutoff in these calculations was 400 eV, and the Brillouin zones were sampled with gamma-centered Monkhorst-Pack meshes of 8x8x2, 12x12x8 and 11x11x11 k-points for the slab models and the ZnO and anatase primitive lattices respectively.

Final structural relaxations and determination of the remaining electronic structure features were carried out using hybrid functionals. Doing this with a plane wave based code as VASP is computationally very demanding in the case of unit cells containing more than few tens of atoms, due to the way in which this type of code computes the exchange terms. Because of this, program CRYSTAL09[31] was used here for all hybrid functional calculations. This program expands wavefunctions and densities as

combinations of atom-centered functions of gaussian shape, which makes less costly the evaluation of the integrals needed to compute the Fock exchange. The basis set used for oxygen was the 8-411d11G basis set reported in ref. 32, and for titanium the 86-411(d31)G basis set of ref. 33 was used, augmented as recommended by Di Valentin et al.[34] with an additional d diffuse function for which an exponent 0.12 was adopted here. For Zn the Stevens' relativistic equivalent core potential (RECP) keeping 20 electrons in the valence space[35] was used, as well as the corresponding basis set given in the same work; however the most diffuse sp function in the latter basis set, which is optimized for molecular systems, had to be changed as it gave rise to linear dependencies and instabilities in the periodic calculations, its exponent being therefore increased from 0.0537 to 0.09, which value proved to minimize the total electronic energy in the calculations with ZnO. In the CRYSTAL09 calculations the Brillouin zone sampling was the same as with VASP. The hybrid functional used was of PBE0 type, but with the fraction α of Hartree-Fock exchange adjusted according to the criteria explained below.

In this work a complication arose because, as explained in the Results section, the known inadequacy of DFT-GGA methods to reproduce experimental band gap values cannot be corrected with a hybrid functional simultaneously for TiO_2 and ZnO, i.e. if the same functional is used for both oxides; it can only give correct results if the fraction α of HF exchange used is higher for ZnO than for TiO_2. That it may be reasonable to use different α values for different oxides can be justified if one considers that, as discussed by Alkauskas et al.[36] and Marques et al.[37], mixing with the DFT functional a fraction (α) of HF exchange reflects the fact that the latter is subjected to a screening which is related to the dielectric properties of the material considered. These works indicate that it is quite reasonable to assume $\alpha=1/\varepsilon_\infty$; the latter authors show in fact that using α values chosen in this way allows obtaining with rather good

approximation the band gap E_g for a series of different semiconductors. As will be shown below, using for both ZnO and anatase α values computed from experimentally obtained ε_∞ values according to this recipe allows to reproduce rather well their experimental band gaps.

However, the problem remains that a calculation on the slab model shown above can use only one α value, leading therefore to error in at least one of the gaps so that the relative band edge positions directly resulting from such calculation cannot be trusted. This problem can be circumvented using the procedure proposed some time ago by Van de Walle and Martin[8] and recently applied also to defect-containing systems by Alkauskas et al.[36]. Essentially, it proposes to use the electrostatic potential inside the solid as a valid common reference level to relate the results of GGA and hybrid functional calculations (or, for that matter, those of hybrid functional calculations using different values of α). This is reasonable if one considers that the electrostatic potential in a solid is computed with equal accuracy by different functionals, at least if the geometry, the basis set used to expand the electronic functions and the pseudopotentials used are kept the same; the differences among the functionals affect then only to the exchange and correlation parts of the potential. The validity of the electrostatic potential as reference for determining the position of electronic levels has been further evidenced in a recent work by Ramprasad et al. [38] showing that the position obtained in a calculation for a defect level in a semiconductor, if referenced to the electronic potential, is practically the same independently of the functional, i.e. of how the exchange-correlation potential is chosen. These authors also propose using the valence band width, rather than the bandgap, as experimental parameter to which the optimum hybrid functional should be fitted, which is certainly an interesting idea. In the case of ZnO the said width, about 5 eV, is hard to determine with accuracy, as the valence band

bottom nearly overlaps the upper part of the 3d band[39]; thus Van de Walle and Martin's criterium of fitting α to the gap for each binary oxide will be followed instead.

Alkauskas et al.[36] propose thus a procedure in which, for each one of the pure phases, the positions of the gap edges respect to the electrostatic potential distribution in the solid are determined through calculations which give the correct bandgap width (using appropriate functionals); then the electrostatic potential distribution in a model of the interface is computed with some functional (hybrid or not) and both results are combined to find out the relative band edge positions of the two materials. This procedure will be followed here, using the CRYSTAL09 program to compute both the distribution of total electrostatic potential in the unit cell and the band positions for different α values.

Results and discussion.

Computing the band gaps of the single oxide phases

As said above, one same functional (with a given α value) is unable to reproduce the band gaps of both anatase and ZnO. For example, mixing into the PBE functional a fraction α=0.20 of HF exchange (the same used in the well-known B3LYP functional) yields with the CRYSTAL09 code, once the structures are fully relaxed in both cell dimensions and atomic coordinates, band gaps of 3.78 eV (indirect) and 2.80 eV (direct) for anatase and ZnO respectively. In both cases increasing α increases E_g and vice versa; one same α value cannot give therefore the correct E_g for both oxides. Thus the relationship $\alpha=1/\varepsilon_\infty$ was used to derive α from ε_∞ values obtained experimentally either from optical properties in the IR range or, using the relationship $\varepsilon=n^2$, from the refractive index at photon energies below the onset of band gap absorption. For anatase

an isotropically averaged value ε_∞=5.68 has been evaluated from IR properties[40] while a value ε_∞=6.44 can be derived from the refractive index, resulting in α=0.176 or 0.155 respectively; for ZnO ε_∞ values of 3.73 and 3.98 have been deduced from IR properties[41] (giving α=0.268 and 0.251 respectively), while the refractive index gives ε_∞=4.0, i.e. α=0.25. Here α=0.165 and 0.26 will be assumed to be acceptable experiment-based values for anatase and ZnO respectively.

The band gaps computed with CRYSTAL09 for both oxides using these α values are 3.49 eV (indirect) for anatase and 3.35 eV for ZnO; these are much closer to the experimental values (at 0 K) mentioned above. This means that there is a sound basis to assume that, at least for this class of oxide semiconductors, it is appropriate to use a mixing coefficient α which is not the same for all systems as it is related to the dielectric screening properties of each material. However, for the purposes of the present work it seems more adequate to use, as proposed in ref. 8, the α value which best reproduces the experimental E_g. Further adjustment leads to α=0.16 for anatase, giving for it E_g=3.43 eV (indirect gap), and α=0.267 for ZnO, which leads to E_g=3.44 eV (direct gap). The density of states curves so obtained are depicted in Fig. 2. These show for ZnO the narrow band of filled Zn 3d states lying just below the valence band, as known from experiment, and verify that the conduction bands of anatase and ZnO are made largely by Ti 3d and Zn 4sp states respectively, with much smaller DOS at the conduction band lower edge in the second case due to its much broader and more delocalized character.

Finally, it can be mentioned that after full structural relaxation the mentioned calculations reproducing the experimental E_g values gave for ZnO and anatase the unit cell parameters and metal-oxygen bond lengths summarized in Table 1. It can be seen that these figures approach rather well the experimental values at near-liquid helium temperatures[42,43] (with which these calculations, which do not include thermal effects,

should be compared), shown also in the Table. Furthermore, these hybrid functional calculations reproduce the experimental geometry significantly better than the calculations made with CRYSTAL09 at the standard DFT-GGA level (with no hybrid mixing of HF exchange), these results being given as well in Table 1.

Modeling the anatase-ZnO interface

The structural model depicted in Fig. 1 was relaxed to obtain the energy minimum, first with VASP using GGA and then, starting with the so relaxed geometry, in a second relaxation with CRYSTAL09 using a hybrid functional in which a value α=0.22 was used, intermediate between those giving the correct E_g values for the two binary oxides. This approach of adopting an intermediate α value, rather than just using the GGA functional as starting point, was considered preferable in order to obtain an overall geometry, and a resulting electron density and electrostatic potential distribution, which are as close as possible to those which would result in an exact calculation and approaches similarly the best description of both oxides. In such slab calculation numerical instabilities preventing scf convergence were found for α values above 0.10 if the most diffuse sp exponent was kept in the Zn basis set; this calculation was therefore carried out without this exponent, but as will be shown below this affects only marginally the essential result sought. It must be said also that this problem appeared only with the slab model calculations, not with those made for the single oxides; it is probably due to the large size of the slab model, i.e. to the c axis length and/or the large number of atoms.

The resulting unit cell, which keeps the initial monoclinic symmetry, had parameters a=5.462 Å, b=5.312 Å, c=39.175 Å and β=90.563º. This is the geometry shown in Fig. 1. Note that these a and b parameters are intermediate between those of the initial ZnO

and anatase lattices, mentioned above. On the other hand the spacings between lattice planes parallel to the interface, measured near the central plane of both oxide slabs, are 1.655 Å and 2.384 Å for ZnO and anatase respectively; these are rather close to the values 1.635 Å and 2.410 Å that result after full relaxation in the calculations using the optimal α value for each phase. On the other hand, although the symmetry of the model allows the atoms at the slabs centers to deviate from their central planes, the observed displacements (from the ideal positions occurring in the pure oxides) in the direction normal to these planes were found to be rather small: negligible for the cations (1.1 x 10^{-4} Å for Zn and 3 x 10^{-4} Å for Ti) and also small for the oxygens (0.01 Å in ZnO and 0.003 Å in anatase), giving a first indication that the situation of the atoms at the slabs centers is representative of that in the bulk, i.e. that the slabs are thick enough.

Concerning the atomic arrangements at the interface, a detailed analysis of the bonding resulting geometries is not of particular interest here, but it may be mentioned that the new bonds formed between the slabs are in the average somewhat longer (most of them have d(M-O)> 2.00 Å) than those found near the slabs centers, and that the ZnO plane closest to the interface becomes more distorted and buckled, reflecting probably the less compact and electrically charged (and consequently more flexible) nature of the ZnO lattice in comparison to the anatase one.

For the estimation of the electronic level positions the electrostatic potential in this relaxed slab model was computed using a grid of spacing d≈0.039 Å and the potential was averaged in each plane of the grid parallel to the interface. The value of such plane-averaged potential, multiplied by the electronic charge, is plotted in Fig. 3a against the lattice coordinate perpendicular to the interface plane; only one half of the cell is represented, as the other half is equivalent by symmetry. The sharp minima corresponding to the atom-containing planes are easily discerned. In the TiO_2 part the

deviations of the O atoms from the Ti-containing equatorial planes, typical of the anatase structure, are reflected in shoulders appearing in the potential profile through the whole anatase layer, and the distortions of the atomic positions at the ZnO side of the interface are also noticeable as shoulders. The values of the plane-averaged potential at the atom containing planes (where the minima appear) are probably not computed at high accuracy with the grid spacing used here, due to the difficulty of an exact integration near the potential cusps occurring at the atom positions; therefore the values which would result from three-dimensional averaging within one lattice period chosen near the center of each slab, proposed in ref. 8 as reference values for the electronic levels, might be computed also with some inaccuracy. For this reason, in this work the 2D-averaged energy value (here designated E_{top}) at the point with zero slope which appears at or near the midpoint between the atomic planes will be taken instead as reference value. It can be seen that the zero slope values oscillate within each slab near the interface, but reach near the slab center a constant value, which is E_{top}=-3.11 eV and -1.07 eV for the ZnO and TiO_2 regions respectively.

The essential result here is the difference between these two values, which amounts to ΔE_{top}=2.04 eV. It is necessary to check if the suppression of the most diffuse sp function in the Zn basis set affects to this value. For this several calculations of ΔE_{top} were made with and without this function, using α values which do not lead to numerical instabilities in the calculation. It was found that ΔE_{top} varies with α slightly and nearly linearly (in particular, when the diffuse function is not used the computed ΔE_{top} is 0.135 eV smaller for α=0.22 than for α=0.0), and that this dependence has nearly the same slope with and without the inclusion of the diffuse function, so that for any α value ΔE_{top} decreases consistently by ca. 0.025 eV when the diffuse function is included. One

may thus assume that including such function with α=0.22 (if the numerical instabilities could be avoided) would lead to a ΔE_{top} value around 2.01 eV.

Then it is necessary to carry out a similar electrostatic calculation for the pure ZnO and TiO_2 phases. But since these are distorted due to the epitaxial strain, in order to ensure a correct picture of the electronic situation the appropriate thing is to obtain this potential as well as the band gap values for the thus distorted structures. Therefore for this calculation the lattice constants and atomic coordinates were taken from the central region of each slab, taking the unit cell defined by the two atomic planes nearest to the central plane of each slab. For the distorted cells obtained in this way (which kept the screw symmetry axis of the full slab model) hybrid functional calculations were carried out without any further relaxation. The same α values as for the undistorted cells were used, considering the very small magnitude of these distortions. The band gaps obtained (including in this case the diffuse sp function of the Zn basis set, as E_g was found to be sensitive to it) were respectively 3.39 eV and 3.43 eV for these distorted ZnO and anatase lattices. Therefore there is a (rather) small change for ZnO due to the epitaxially induced distortion, but nearly none for anatase.

The electrostatic potential profile obtained in this way for both slightly distorted lattices is depicted in Fig. 3b, which includes for each one together with the E_{top} position the locations of the valence and conduction band edges. By transferring the separations between E_{CB} and E_{top} from these results to the situation depicted in Fig. 3a the final result is obtained that at the interface between anatase and ZnO the conduction band of the former oxide is located some 0.35 eV higher than that of ZnO; if one assumes the above mentioned value ΔE_{top}=2.01 eV expected for a calculation including the diffuse sp function, the difference is slightly modified, becoming 0.32 eV. The difference in the positions of the valence band edges is very similar: 0.28 eV, in agreement with the

slight difference in bandgaps. Since the effects of the epitaxially induced distortion are rather small, as explained above, one may assume that a very similar alignment would occur in any contact between ZnO and anatase in which no bulk lattice distortion exists, at least if no polar surfaces are involved and interface-induced local distortions are not too large. To check the convergence of this result with the slab model size additional calculations were carried out on a smaller model having 5 anatase layers and 7 ZnO layers (instead of 9 and 11) in the respective slabs, being otherwise identical (same surfaces forming the interface, same bonds being established and same global symmetry). The energy difference between both conduction bands found in this case through the same procedure (using a Zn basis set without the diffuse sp function, as the latter gave rise to instabilities also in this case) was 0.45 eV (of the same sign). The slightly different value found for the energy difference in the 5+7 layers model could be due to the presence in the latter of a residual interaction (electrostatic or elastic) between the two interfaces; but the fact that almost doubling the model size from 5+7 to 9+11 layers modified the result in only 0.1 eV gives confidence that a model with still thicker slabs would leave the result essentially unchanged. Indeed slab models used in the literature for modeling this type of oxides[44] have typically thicknesses not higher than those shown in Fig. 1. Also a model with 9+9 layers gave practically the same result as the 9+11 model, confirming that changing the proportion between the slabs thicknesses does not modify the effect.

The situation can be thus summarized as depicted schematically in Fig. 4, where the feature most important for photocatalysis is revealed: if an electron-hole pair is formed by photon absorption at any of both oxides, the interface will favor charge separation so that the electron will tend to be located at the ZnO side while the hole will be located at the anatase side, at least while the additional electric field generated by this charge

separation is not enough to counteract the difference of levels. Thus one may expect that in a photocatalytic system based on this type of composite the chemical processes resulting from the transfer of holes to the surrounding fluid will be more similar to those occurring on TiO_2, while those resulting from the transfer of the photogenerated electrons will be more similar to those typical for ZnO. Of course one may hypothesize additionally that photons having an energy lower by ≈0.3 eV than the band gap widths of both oxides could be absorbed at the interface position, accompanied by direct electron transfer across it, leading to some photocatalytic activity with visible light; the importance of this phenomenon will depend however on the extent of the ZnO-anatase interface and on the corresponding absorption coefficient magnitude.

In addition one may note that this band alignment situation can have also an effect in dye- or quantum dot-sensitized photovoltaic cells if these include a combination of both oxides in the electrode collecting the electron current. In fact, recent results[45] have shown that one such cell in which the said electrode is made of ZnO increases significantly its efficiency if a very thin anatase layer is deposited on the ZnO surface prior to adsorbing the dye. It was interpreted in that work that by doing this the recombination between the electrons injected in the electrode and the oxidized dye was strongly decreased; such effect can be cleanly explained with the present results, which predict that the electrons initially injected in the external TiO_2 layer would be quickly transferred to the underlying ZnO, and being thus spatially separated from the adsorbed dye (which keeps the hole before transferring it to the liquid) the mentioned recombination would be impeded.

Finally it may be noted that the procedure followed here can be extended to other combinations of semiconductors (in photocatalysis or in other applications) for which one needs to clarify the band alignment. If the corresponding band gaps are known, the

mixing coefficient α should be fitted in each individual semiconductor calculation to reproduce the gap, otherwise both parameters (band gap and α value) can be estimated from a theoretical evaluation of ε_∞, which can be done e.g. using the CPHF/KS[46] or TD-DFT[37] theoretical approaches. Of course, the α values chosen according to these criteria might not be the best ones for reproducing other properties like cohesive energies, magnetism or vibrational spectra; here the concern is however about electronic levels, as required by the Van der Walle and Martin's procedure, and according to the results above the said criteria give good results in this respect. Finally it may be mentioned that, at least for the calculations on the binary oxides, the band edge positions relative to the electrostatic potential can be alternatively estimated using GW theory (even if the latter is still computationally rather expensive), and coupling this to a potential distribution estimation made with standard DFT can yield a fully first principles determination of band alignment.[47] Further development of this approach in the future could provide an accurate method of band offset prediction.

Conclusions

Using careful procedures which take into account the need of using appropriate exchange mixing coefficients in hybrid functional calculations, as well as theoretically justified relationships between these coefficients and dielectric properties and between the band positions and the electrostatic potential distribution, it is possible to determine with reasonable reliability using hybrid density functional theory the band alignments present at the interfaces between semiconductors. When applied to ZnO-TiO_2 composite photocatalysts, as done here, this allows determining that the bands of ZnO will lie a few tenths of eV (around 0.3 eV) lower than those of anatase; one can then analyze how charge transfer effects may occur at these interfaces, which will influence the evolution

of photocatalytic reactions and probably also the behavior of photovoltaic devices when such interfaces are present in them. Although strictly speaking the calculations describe a situation at a temperature near 0 K, the alignment of bands in the system is expected to remain essentially the same at ambient temperature, since in those conditions the band gaps of both oxides are, although somewhat smaller, still of similar magnitude.

Acknowledgement

This work was pursued with financial help from national project FOTOMAT (ref. nr. MAT2009-14625), regional project NUMANCIA-2 (ref. nr. S2009ENE-1477) and COST action 540 PHONASUM, and used the CTI computing infrastructure of the CSIC; to all of them thanks are given here. Thanks are expressed also to Dr. Lubomir Spanhel for suggesting the interest of a theoretical analysis of the ZnO-TiO_2 photocatalytic system.

References

[1] Kraut, E.; Grant, R.; Waldrop, J.; Kowalczyk, S. *Phys. Rev. Lett.* **1980**, *44*, 1620-1623; *ibid. Phys. Rev. B* **1983**, *28*, 1965-1977.

[2] Itzhaik, Y**.;** Hodes, G.; Cohen, H. *J. Phys. Chem. Lett*. **2011**, *2*, 2872-2876.

[3] Perego, M.; Seguini, G. *J. Appl. Phys*. **2011**, *110*, 053711-1 – 053711-11.

[4] Yamakawa, I.; Akanuma, Y.; Akimoto, R.; Nakamura, A. *Appl. Phys. Lett.* **2005**, *86*, 153112-1 – 153112-3.

[5] Chien, T. Y.; Liu, J. A.; Chakhalian, J.; Guisinger, N. P.; Freeland, J. W. *Phys. Rev. B* **2010**, *82*, 041101-1 – 041101-4.

[6] Dietmüller, R.; Nesswetter, H.; Schöll, S. J.; Sharp, I. D.; Stutzmann, M. *ACS Appl. Mater. Interf.* **2011**, *3*, 4286-4291.

[7] Chen, A.; Woodall, J. M. *Appl. Phys. Lett.* **2009**, *94*, 021102-1 – 021102-3.

[8] Van de Walle, C. G.; Martin, R. M. *Phys. Rev. B* **1987**, *35*, 8154-8165.

[9] Moses, P. G.; Miao, M.; Yan, Q.; Van de Walle, C. G. *J. Chem. Phys.* **2011**, *134*, 084703-1 – 084703-11.

[10] Van de Walle, C. G.; Neugebauer, J. *Nature* **2003**, *423*, 626-628.

[11] Giantomassi, M.; Stankovski, M.; Shaltaf, R.; Grüning, M.; Bruneval, F.; Rinke, P.; Rignanese, G.-M. *Phys. Status Solidi B* **2011**, *248*, 275-289.

[12] Kubacka, A.; Fernández-García, M.; Colón, G. *Chem. Rev*. **2012**, *112*, 1555-1614.

[13] Ravelli, D.; Dondi, D.; Fagnoni, M.; Albini, A. *Chem. Soc. Rev*. **2009**, *38*, 1999-2011.

[14] Tang, H.; Levy, F.; Berger, H.; Schmid, P. E. *Phys. Rev. B* **1995**, *52*, 7771-7774.

[15] Mang, A.; Reimann, K.; Rübenacke, S. *Solid State Communications* **1995**, *94*, 251-254.

[16] Marcí, G.; Augugliaro, V.; López-Muñoz, M. J.; Martín, C.; Palmisano, L.; Rives, V.; Schiavello, M.; Tilley, R. J. D.; Venezia, A. M. *J. Phys. Chem. B* **2001**, *105*, 1033-1040.

[17] Shifu, C.; Wei, Z.; Wei, L.; Sujuan, Z. *Appl. Surf. Sci.* **2008**, *255*, 2478-2484.

[18] Zhang, Z.; Yuan, Y.; Fang, Y.; Liang, L.; Ding, H.; Jin, L. *Talanta* **2007**, *73*, 523-528.

[19] Jiang, Y.; Sun, Y.; Liu, H.; Zhu, F.; Yin, H. *Dyes and Pigments* **2008**, *78*, 77-83.

[20] Liao, S.; Huang, D.; Yu, D.; Su, Y.; Yuan, G. *J. Photochem. Photobiol. A* **2004**, *168*, 7-13.

[21] Khalyavka T. A.; Khalyavka, T. A; Kapinus, E. I.; Viktorova, T. I.; Tsyba, N. N. *Theor. Exp. Chem.* **2009**, *45*, 234-238.

[22] Karunakaran, C.; Dhanalakshmi, R.; Gomathisankar, P.; Manikandan, G. *J. Hazardous Mater.* **2010**, *176*, 799-806.

[23] Panigrahi, S.; Basak, D. *Nanoscale* **2011**, *3*, 2336-2341.

[24] Lin, H. Y.; Chou, Y. Y.; Cheng, C. L.; Chen, Y. F. *Optics Express* **2007**, *15*, 13832-13937.

[25] Wang, M.; Huang, C.; Cao, Y.; Yu, Q.; Deng, Z.; Liu, Y.; Huang, Z.; Huang, J.; Huang, Q.; Guo, W. *et al. J. Phys. D: Appl. Phys*. **2009**, *42***,** 155104-1 – 155104-6.

[26] Liu, R.; Ye, H.; Xiong, X.; Liu, H. *Materials Chemistry and Physics* **2010**, *121*, 432-439.

[27] Wang, J.; Liu, X.-L.; Yang, A.-L.; Zheng, G.-L.; Yang, S.-Y.; Wei, H.-Y.; Zhu, Q.-S.; Wang**,** Z.-G. *Appl Phys A* **2011**, *103*, 1099-1103.

[28] See e.g. Zhang, Z.; Meng, G.; Xu, Q.; Hu, Y.; Wu, Q.; Hu, Z. *J. Phys. Chem. C* **2010,** *114*, 189-193.

[29] Kresse, G.; Hafner, J. *Phys. Rev. B* **1993**, *47*, 558-561.

[30] a) Blöchl, P. E.; *Phys. Rev. B* **1994**, *50*, 17953-17979; b) Kresse, G.; Joubert, J. *Phys. Rev. B* **1999**, *59*, 1758-1775.

[31] Dovesi, R.; Saunders, V. R.; Roetti, C.; Orlando, R.; Zicovich-Wilson, C. M.; Pascale, F.; Civalleri, B.; Doll, K.; Harrison, N. M.; Bush, I. J. *et al.*, CRYSTAL09 User's Manual, Università di Torino (Torino, 2010).

[32] Valenzano, L.; Torres, F. J.; Klaus, D.; Pascale, F.; Zicovich-Wilson, C. M.; Dovesi, R. *Z. Phys. Chem.* **2006**, *220*, 893-912.

[33] Corá, F. *Mol. Phys.* **2005**, *103*, 2483-2496.

[34] Di Valentin, C.; Finazzi, E.; Pacchioni, G.; Selloni, A.; Livraghi, S.; Czoska, A. M.; Paganini, M. C.; Giamello, E. *Chem. Mater.* **2008**, *20*, 3706-3714.

[35] Stevens, W. J.; Krauss, M.; Basch, H.; Jasien, P. G. *Can. J. Chem.* **1992**, *70*, 612-630.

[36] Alkauskas, A.; Broqvist, P.; Pasquarello, A. *Phys. Status Solidi B* **2011**, *248*, 775-789.

[37] Marques, M. A. L.; Vidal, J.; Oliveira, M. J. T.; Reining, L.; Botti, S. *Phys. Rev. B* **2011**, *83*, 035119-1 – 035119-5.

[38] Ramprasad, R.; Zhu, H.; Rinke, P.; Scheffler, M. *Phys. Rev. Lett.* **2012**, *108*, 066404-1 – 066404-5.

[39] Didziulis, S. V.; Cohen, S. L.; Butcher, K. D.; Solomon, E. I. *Inorg. Chem.* **1988**, *27*, 2238-2250.

[40] Gonzalez, R. J.; Zallen, R.; Berger, H. *Phys. Rev. B* **1997**, *55*, 7014-7017.

[41] a) Ooi, P.; Lee, S.; Ng, S.; Hassan, Z.; Abu Hassan, H. *J. Mater. Sci. Technol.* **2011**, *27*, 465-470; b) Venger, E. F.; Melnichuk, A. V.; Melnichuk, L. Y.; Pasechnik, Y. A. *Phys. Status Solidi (b)* **1995**, *188*, 823-831.

[42] Yoshio, K.; Onodera, A.; Satoh, H.; Sakagami, N.; Yamashita, H. *Ferroelectrics* **2001**, *264*, 133-138.

[43] Burdett, J. K.; Hughbanks, T.; Miller, G. J; Richardson Jr., J. W.; Smith, J. V., *J. Amer. Chem. Soc*. **1987**, *109*, 3639-3646.

[44] Ganduglia-Pirovano, M. V.; Hofmann, A.; Sauer, J. *Surf. Sci. Rep.* **2007**, *62*, 219-270.

[45] Tétreault, N.; Arsenault, É.; Heiniger, L.-P.; Soheilnia, N.; Brillet, J.; Moehl, T.; Zakeeruddin, S.; Ozin, G. A.; Grätzel, M. *Nano Lett*. **2011**, *11*, 4579-4584.

[46] Ferrero, M.; Rérat, M.; Orlando, R.; Dovesi, R. *J. Chem. Phys*. **2008**, *128*, 014100; *ibid. J. Comput. Chem*. **2008**, *29*, 1450-1459.

[47] a) Shaltaf, R.; Rignanese, G.-M.; Gonze, X.; Giustino, F.; Pasquarello, A. *Phys. Rev. Lett.* **2008**, *100*, 186401-1 – 186401-4; b) Mitra, C.; Lange, B.; Freysoldt, C.; Neugebauer, J. *Phys. Rev. B* **2011**, *84*, 193304-1 – 193304-4.

Figure captions

Figure 1- Periodic slab model, with a total content of stoichiometry $Zn_{22}Ti_{18}O_{58}$ in the unit cell, used to study the interface between ZnO(110) and anatase-type TiO_2(001). The twofold screw axis of symmetry is near-perpendicular to the drawing plane.

Figure 2- Density of states curves around the bandgap (total and projected on the cations) computed for anatase and ZnO using respectively α=0.16 and 0.267 in the hybrid functional. For ZnO the total DOS is plotted also magnified by a x5 factor to better appreciate the conduction band bottom edge.

Figure 3- a) Electrostatic potential (multiplied by the electron charge) computed with α =0.22 for the slab model and averaged in a plane parallel to the layers, plotted against the third coordinate; only 50% of the unit cell is represented. b) Same quantity computed for TiO_2 and ZnO with same geometry as in the central part of the slabs, using in each case the optimal α value; the valence and conduction band positions are noted as well

Figure 4- Scheme, according to the calculations, of the relative positions of the conduction and valence bands of anatase and ZnO in contact, depicting the hole and electron charge separation across the interface.

Table 1– Cell dimensions and M-O bond lengths (in Å) calculated for ZnO and anatase-TiO_2 with GGA and hybrid DFT methods, compared to experimental results

		exptl. (at T<20 K)	hybrid DFT	GGA
anatase			(α=0.16)	
	a	3.782	3.790	3.815
	c	9.502	9.640	9.720
	$d(Ti\text{-}O)_c$ [a]	1.978	1.987	2.006
	$d(Ti\text{-}O)_{ab}$ [a]	1.932	1.942	1.954
ZnO			(α=0.267)	
	a	3.247	3.270	3.304
	c	5.203	5.197	5.275
	$d(Zn\text{-}O)_c$ [a]	1.983	1.998	2.020
	$d(Zn\text{-}O)_{ab}$ [a]	1.974	1.981	2.005

[a] $d(M\text{-}O)_c$ and $d(M\text{-}O)_{ab}$ refer to M-O bonds lying respectively parallel and oblique (near perpendicular, in the anatase case) to the c axis of the crystal cell

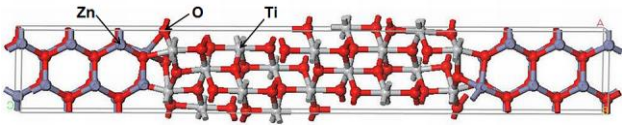

Figure 1- Periodic slab model, with a total content of stoichiometry $Zn_{22}Ti_{18}O_{58}$ in the unit cell, used to study the interface between ZnO(110) and anatase-type TiO_2(001). The twofold screw axis of symmetry is near-perpendicular to the drawing plane.

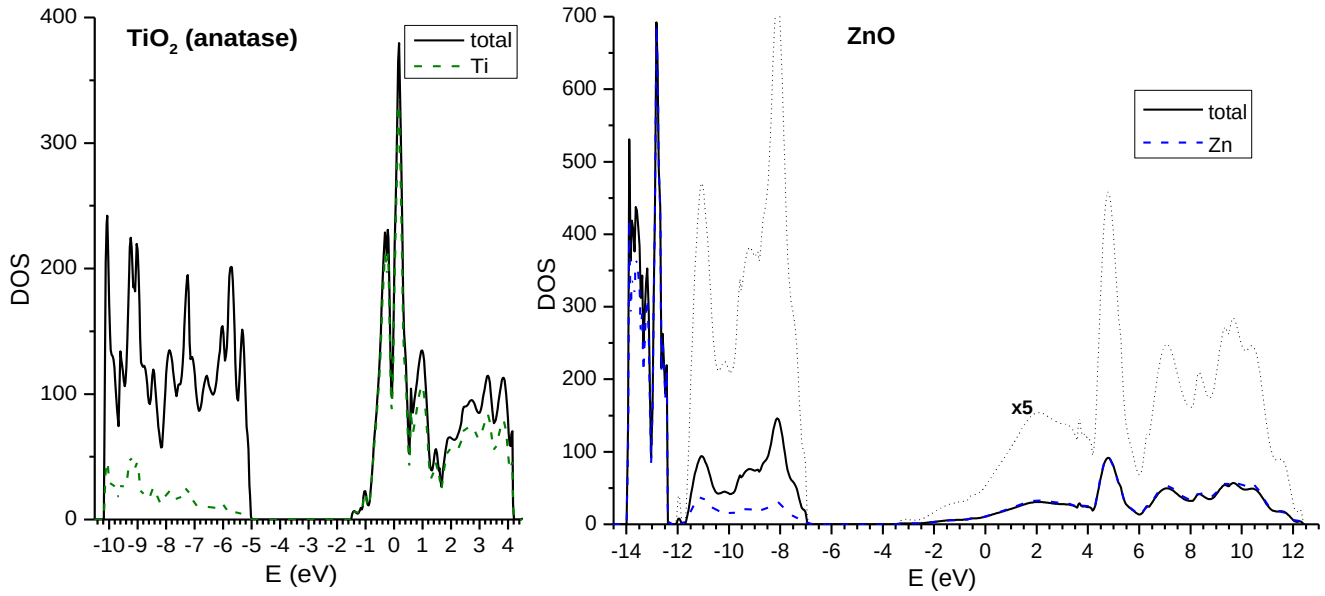

Figure 2- Density of states curves around the bandgap (total and projected on the cations) computed for anatase and ZnO using respectively α=0.16 and 0.267 in the hybrid functional. For ZnO the total DOS is plotted also magnified by a x5 factor to better appreciate the conduction band bottom edge.

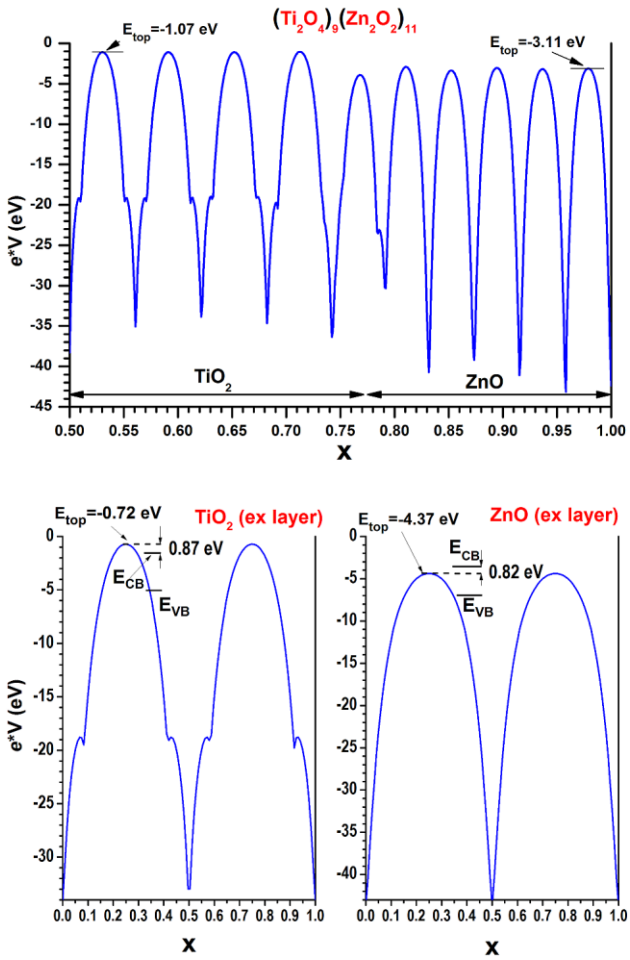

Figure 3- a) Electrostatic potential (multiplied by the electron charge) computed with α =0.22 for the slab model and averaged in a plane parallel to the layers, plotted against the third coordinate; only 50% of the unit cell is represented. b) Same quantity computed for TiO_2 and ZnO with same geometry as in the central part of the slabs, using in each case the optimal α value; the valence and conduction band positions are noted as well.

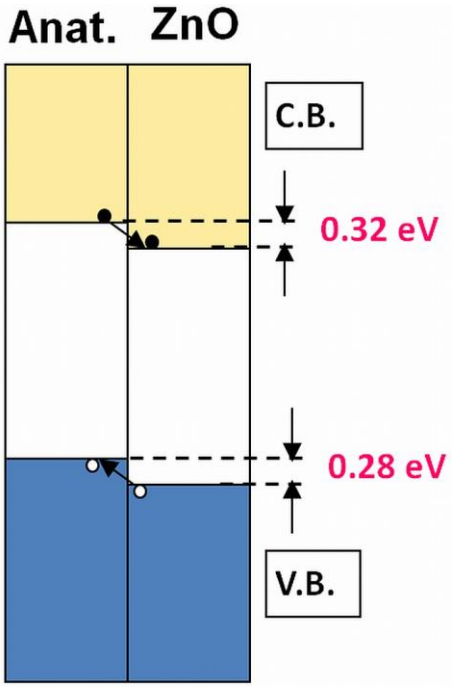

Figure 4- Scheme, according to the calculations, of the relative positions of the conduction and valence bands of anatase and ZnO in contact, depicting the hole and electron charge separation across the interface.

Table of contents image